Dual Polarized Reflectarray Transmit Antenna for Operation in Ku- and Ka-Bands With Independent Feeds

Eduardo Martinez-de-Rioja, Jose A. Encinar, Mariano Barba, Rafael Florencio, Rafael R. Boix, and Vicente Losada

***Abstract*— A reflectarray antenna capable of operating independently in the transmit frequencies (from a satellite) in Ku-band (11–13 GHz) and Ka-band (19–20 GHz) has been proposed and demonstrated. To prove that independent beams can be optimized in each frequency band using separate feeds, a 25-cm demonstrator that generates a focused beam in dual polarization (linear or circular) has been designed, manufactured, and tested. The reflectarray cells comprise two stacked sets of coupled parallel dipoles for each polarization, which permits an independent optimization of the phase for each frequency and polarization. The simulated and measured radiation patterns for both copolar and cross-polar components are in good agreement in Ku- and Ka-bands.**

***Index Terms*— Communications satellites, coupled dipoles, dual frequency, dual polarization, reflectarrays.**

I. Introduction

Reflectarray antennas are composed of many radiating elements printed on a flat reflecting surface, with an illuminating feed antenna. The elements reradiate the incident field from the feed with a certain phase shift, in order to generate collimated or contoured beams [1]. Thanks to the use of planar reflective surfaces instead of shaped curved reflectors, reflectarrays have become a potential alternative for space antennas in satellite systems working in Ku- and Ka-bands [2].

Telecommunications satellites require an increasingly larger number of antennas to provide fixed services in Ku-band and broadband access in Ka-band [3]. A major trend is to accommodate multiple payloads for different functions in the satellite. For example, the reuse of the same main reflector for Ku and Ka missions by a dichroic subreflector [4] to separate the feed chains in each frequency band will provide a significant saving of space in the satellite.

The flexibility of reflectarray antennas to generate independent beams in each frequency and polarization [5] can be used to design a reflectarray to fulfill independent requirements in Ku- and Ka-bands. Several papers have been reported for dual-frequency reflectarrays. There are two basic strategies of design: either different resonant elements distributed on a single layer are used [6], [7], or a stacked multilayer configuration is employed in which each reflectarray layer operates at a different frequency [8]–[10]. In the first case, the reflectarray cannot operate independently at each polarization. For example, the reflectarray cells made of a split loop combined with a Malta cross [7] work in single circular polarization (CP) at each frequency. On the other hand, a dual-band reflectarray has been developed by placing a Ka-band reflectarray on top of an *X*-band reflectarray, and using a frequency selective surface (FSS) as separator [9], [10]. However, despite the results of these works are satisfactory, the antenna presents a very thick structure with a large number of layers.

The reflectarray element employed in this communication is based on a two layer cell composed of two orthogonal groups of coupled dipoles. The idea of placing two orthogonally arranged sets of coupled dipoles printed on the same layer, but shifted half-a-period, has been used for the design of broadband reflectarrays in Ku-band with independent phase control in each polarization [11]. A latter modification of the cell, which consists of adding a second level of metallization with parallel dipoles, was recently proposed [12], [13] to demonstrate the capabilities of reflectarrays to provide independent phase control in each polarization at two frequencies.

The aim of this communication is to propose and demonstrate a reflectarray antenna capable of operating independently in the transmit frequencies (from a satellite) in Ku-band (11–13 GHz) and Ka-band (19–20 GHz). This concept can be applied to design a satellite transmit reflectarray antenna, which is optimized to fulfill the requirements for two simultaneous missions in Ku- and Ka-bands, considering different feed chains for each mission. For example, a contoured beam can be generated in Ku-band by optimizing the dipole lengths in the lower layer as in [11], and at the same time, multiple spots can be obtained in Ka-band by optimizing the dipoles on the upper layer [14], having more room to properly accommodate the feed chains of each mission. These applications will require a large reflectarray antenna (around 1.5 m diameter). As a proof of concept, a limited sized demonstrator that generates a focused beam in dual polarization using different feeds for Ku- and Ka-bands has been designed, manufactured, and tested.

The proposed reflectarray permits an independent optimization of the radiation patterns and position of feed chains for spacecraft transmit antennas in Ku- and Ka-bands, but similar reflectarray cells can be designed to operate in the receive frequencies (13.75–14.80 GHz in Ku-band and 29–30 GHz in Ka-band). Although this technology obliges to separate transmit and receive antennas, the reuse of the same aperture for Ku and Ka missions would result in significant savings in the costs, weight, and volume of the antenna systems in communication satellites.

II. Reflectarray Element

The unit cell used to provide the phasing in the reflectarray, shown in Fig. 1, is composed of two orthogonal arrangements of eight parallel dipoles, which are distributed on a two-layer configuration: there are five dipoles on the lower layer (A), and three stacked dipoles on the higher layer (B). The symmetry is maintained for the dipoles which are edge coupled to the central dipole of each set so as to ensure a lower level of cross-polar radiation. This configuration has

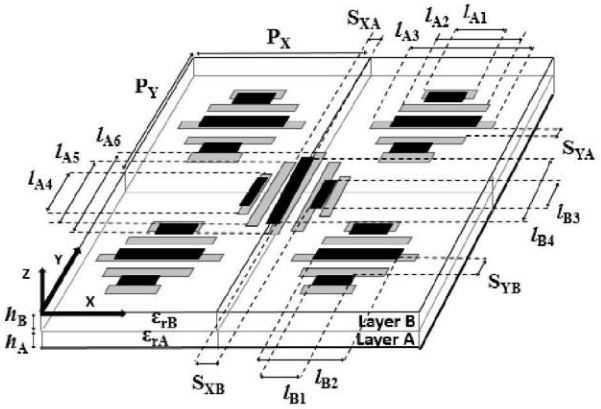

Fig. 1. View of the reflectarray periodic structure, including four unit cells for horizontal polarization and one unit cell for vertical polarization.

been selected with the aim of providing independent phasing in dual polarization at two different design frequencies. The phase introduced in horizontal (H) polarization will be controlled by the lengths of the dipoles in the direction of the x-axis, whereas the phase in vertical (V) polarization will be achieved with the appropriate lengths of the dipoles in the direction of the y-axis. Similarly, the dipoles on the lower layer will adjust the phases in Ku-band, while the dipoles on the higher layer will provide the phases in Ka-band. Since the dipoles on the higher layer are shorter than those on the lower layer, the phase response of the unit cell at the lower frequency (12 GHz) will not be affected by the length of the upper dipoles, and the same applies for the phase response at the higher design frequency (19.5 GHz) regarding the length of the lower dipoles.

A homemade electromagnetic code that applies the method of moments in the spectral domain (MoM-SD) is used for the analysis of the reflectarray cells in a periodic environment [15]. It computes the reflection matrix of each cell, $\boldsymbol{\Gamma}$, formed by the copolar (Γ_{HH} and Γ_{VV}) and cross-polar (Γ_{HV} and Γ_{VH}) coefficients that relate the tangential components of the incident electric field in the direction of dipoles with the tangential components of the reflected field.

A period of 10 mm (which is $2\lambda/3$ at 20 GHz) has been selected for the horizontal (P_X) and vertical (P_Y) dimensions of the cell. This period has been chosen to provide both enough room for the dipoles and enough range of phase shift in the lower band and, at the same time, to avoid grating lobes as much as possible in the higher band. The following relations between the lengths of side and central dipoles have been considered: $l_{A1} = 0.59 \cdot l_{A3}$, $l_{A2} = 0.75 \cdot l_{A3}$, $l_{A4} = 0.59 \cdot l_{A6}$, $l_{A5} = 0.75 \cdot l_{A6}$, $l_{B1} = 0.8 \cdot l_{B2}$, and $l_{B3} = 0.8 \cdot l_{B4}$. The width of the dipoles is 0.5 mm, and the edge-to-edge separations are $S_{XA} = S_{YA} = 0.5$ mm and $S_{XB} = S_{YB} = 1.5$ mm. These parameters were selected after a careful parametric study of the cell, seeking for a linear behavior of the phase response at both design frequencies. The electrical properties and thickness of the two dielectric sheets are: $\varepsilon_{rA} = 2.55$, $\varepsilon_{rB} = 2.17$, $\tan\delta_A = \tan\delta_B = 0.0009$, $h_A = 2.363$ mm, and $h_B = 1.524$ mm.

The reflection coefficients Γ_{HH} and Γ_{VV} (related to each linear polarization) have been computed at different frequencies in Ku- and Ka-bands. Fig. 2 shows the obtained results for $|\Gamma_{HH}|$ and $\arg(\Gamma_{HH})$ under oblique incidence ($\theta_i = 20°$ and $\varphi_i = 0°$) with both nominal and corrected values of ε_r and $\tan\delta$ of the substrates (see Section IV), as the lengths of the dipoles in the direction of x-axis are increased. The graphics only indicate the lengths of the central dipoles (l_{A3} and l_{B2}), but note that the rest of the dipoles are

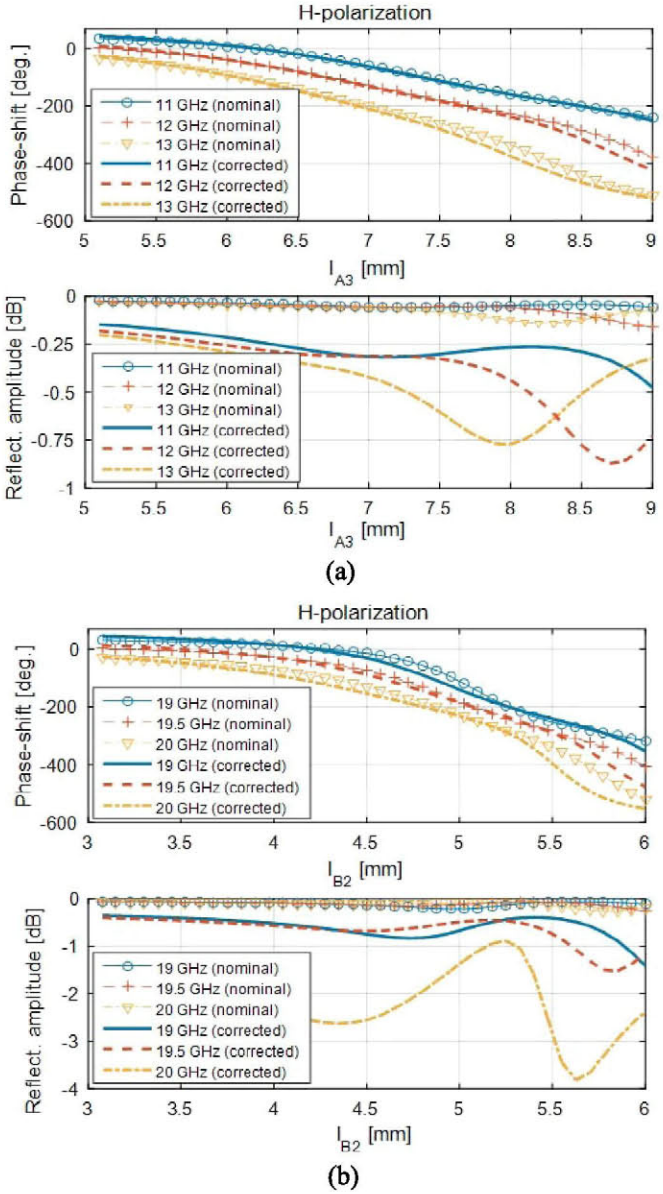

Fig. 2. Magnitude and phase of the cell reflection coefficient, considering H-polarization and $\theta_i = 20°$ incidence at (a) Ku-band and (b) Ka-band.

also varied, while keeping the relations given earlier. The phase shows a fairly smooth variation (almost linear at the lower frequencies) in a 400° interval, which comprises the required 360° margin for the design of the reflectarray. Similar curves are achieved for the orthogonal polarization, considering the lengths of the dipoles in the direction of y-axis.

The orthogonal dipoles placed on the same layer are practically uncoupled as was demonstrated in [11]. So, their lengths can be separately adjusted for controlling the phase response in each linear polarization. In this case, mutual coupling between parallel dipoles in contiguous layers represents the main challenge for achieving independent phase control at each design frequency. Fig. 3 shows the variation in phase of Γ_{HH} and Γ_{VV} with respect to the lengths of upper and lower dipoles in the corresponding directions, at 12 and 19.5 GHz for $\theta_i = 20°$, $\varphi_i = 0°$ angles of incidence.

As can be observed, the element phase response at 12 GHz can be completely controlled by the lengths of the lower dipoles, which means that the design of the bottom layer at 12 GHz can be carried out without considering the dipoles on the higher layer. However, this

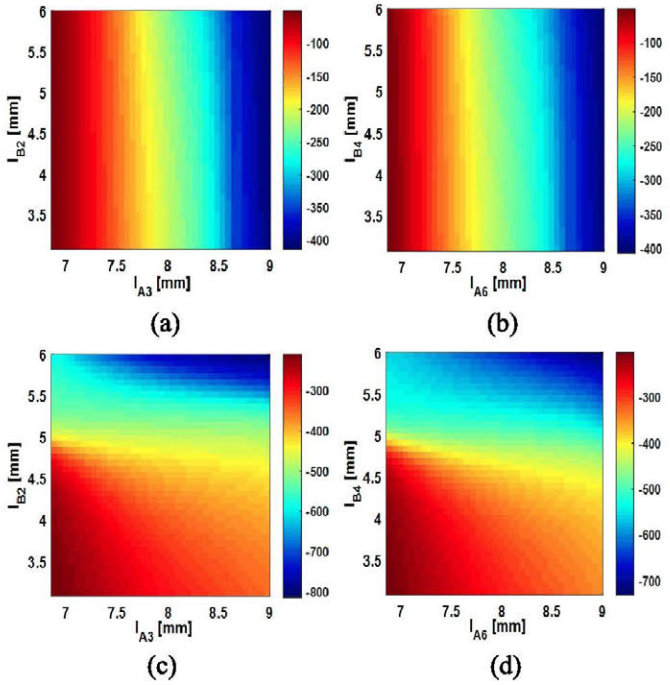

Fig. 3. Phase of the cell reflection coefficient with respect to the lengths of the dipoles in layers A and B, at 12 GHz for (a) H-polarization and (b) V-polarization; and at 19.5 GHz for (c) H-polarization and (d) V-polarization.

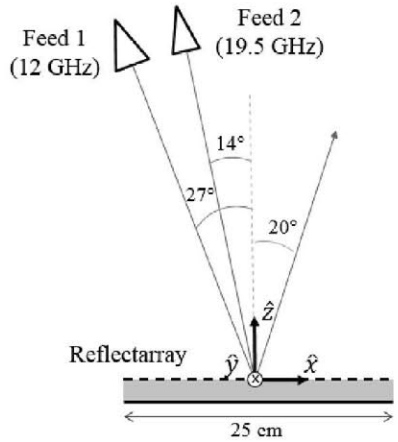

Fig. 4. Schematic of the reflectarray and the two feed-horns in the symmetry plane ($y = 0$).

is not exactly true for the design of the higher layer at 19.5 GHz, since there is certain dependence between the lengths of upper dipoles and the lengths previously calculated for the lower ones, which may slightly affect the phase response of the element. Despite this fact, once the lower layer dimensions have been fixed, there is still enough phase range to implement the required phases at 19.5 GHz with the lengths of upper dipoles.

III. Dual Frequency Design of a Limited Demonstrator

A Ku-/Ka-band reflectarray demonstrator, comprising 625 elements disposed in a 25×25 grid (250-mm sided antenna), has been designed by using the element characterized in Section II. The reflectarray will produce a collimated beam in dual polarization at 12 and 19.5 GHz. The beam will radiate in the direction $\theta_b = 20°$ and $\varphi_b = 0°$ at both design frequencies. Two pyramidal feed horns have been employed to illuminate the antenna in an offset

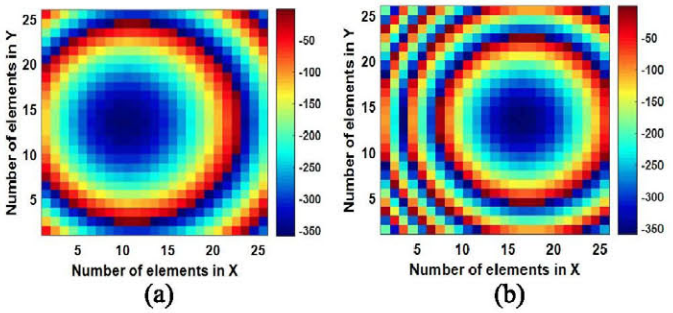

Fig. 5. Required phases to be implemented on the reflectarray surface in H and V polarizations at (a) 12 and (b) 19.5 GHz.

configuration. According to the reference system shown in Fig. 4, the phase centers of the horns are located at the following coordinates: $(x_1, y_1, z_1) = (-114, 0, 223)$ mm for Ku-band horn; and $(x_2, y_2, z_2) = (-62, 0, 247)$ mm for Ka-band horn. The angle of radiation has been chosen to avoid blockage from the feeds, and also to maintain an intermediate value between the angles subtended by the two horns and the z-axis from the reflectarray center, which are 14° and 27° (see Fig. 4). Conventional $\cos^q(\theta)$ functions, based on electromagnetic (EM) simulations of both horns, have been used to model their radiation patterns. The Ku-band horn (VT140SGAH15SK from Vector Telecom), with a gain at 12 GHz of 14.47 dBi and a 3-dB beamwidth of 30°, is modeled with $q = 10$. The gain at 20 GHz for the Ka-band horn (NARDA 638) is 15.6 dBi, the 3-dB beamwidth is 26.7°, and $q = 13$. Under these conditions, the following illumination levels are reached on the reflectarray edges: −9.8 dB at 12 GHz and −13.8 dB at 19.5 GHz.

The phase-shift distributions required on the reflectarray to generate a collimated beam in the specified direction at 12 and 19.5 GHz are shown in Fig. 5 for both polarizations. Since the antenna is designed to provide the same radiation pattern for the two orthogonal components of the incident field, it will operate in dual circular polarization when illuminated by a dual-CP polarized feed. This flexibility may be particularly useful for a multimission space antenna, as most of Ku-band transponders operate in linear polarization, while circular polarization is commonly employed in Ka-band transponders.

The MoM-SD code is employed to obtain the appropriate lengths for each arrangement of dipoles, accounting for the real incidence angle in each cell. First, the required phases at 12 GHz are implemented by considering only the elements on layer A, i.e., the lengths l_{A1} to l_{A3} are varied to control H-polarization, and the lengths l_{A4} to l_{A6} are varied to control V-polarization. Once the lower layer dimensions have been fixed, the required phases at 19.5 GHz are accomplished by adjusting the elements on layer B in a similar way: the lengths l_{B1} and l_{B2} are varied to control H-polarization, and the lengths l_{B3} and l_{B4} are varied to control V-polarization. This step-by-step method simplifies the design of the antenna and reduces the CPU time. The single-frequency design [13] provides acceptable results for the radiation patterns at both design frequencies; however, an additional optimization has been run in order to correct residual phase errors and to ensure the required bandwidth in Ku- and Ka-bands. This process involves the fine tuning of the lengths previously calculated, with the aim of fitting not only the required phases at the central design frequencies, but also the phases at the extremes of both operating bands: 2-GHz bandwidth is enforced in Ku-band (11–13 GHz, 16%), and 1-GHz bandwidth in Ka-band (19–20 GHz, 5.2%). The dipoles in the direction of the x- and y-axes can be independently optimized due to the absence of coupling between the phases of the two orthogonal polarizations, thus simplifying the whole optimization process [11].

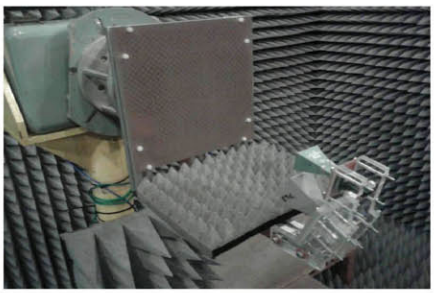

Fig. 6. Reflectarray prototype and measurement setup.

IV. Manufacturing and Measurement

The designed reflectarray antenna has been manufactured and measured. An aluminum structure has been built to sustain the reflectarray, which includes an arm with methacrylate supports to fix the two feed horns. The two levels of printed dipoles are produced by conventional chemical photoetching process. The dipoles are printed on both sides of a DiClad 880 substrate cladded with 17-μm copper. The dielectric layer with the printed dipoles has been bonded to an AD255C sheet backed by the ground plane by using a thermoplastic film (CuClad 6250). Then, the antenna has been fixed to the aluminum supporting plate by means of nylon screws which are placed near the corners of the reflectarray surface.

The manufactured reflectarray antenna (see Fig. 6) has been tested at the anechoic chamber of the University of Seville, in a spherical near-field measurement system. The dimensions of the printed dipoles were checked before the measurement of the antenna, and this test showed that there had been an averaged error of 50 μm in excess in all the lengths and widths of the dipoles of both layers, plus a random error of ± 10 μm. This tolerance error was taken into account in the calculation of numerical radiation patterns, showing that it can lead to a reduction in gain of about 1 dB in Ka-band frequencies, while the effects in Ku-band are almost negligible.

The comparison between the measured and simulated radiation patterns at 12 and 19.5 GHz is presented in Figs. 7 and 8. The patterns show the copolar and cross-polar components for the two linear polarizations in the principal planes: the one tilted 20° with respect to the z-axis (azimuth) and the xz plane (elevation). The MoM-SD code has been used to calculate the tangential components of the reflected electric and magnetic fields on the reflectarray surface. Then, the numerical radiation patterns have been derived from these components.

Fig. 7 shows a quite good agreement between experimental and simulated radiation patterns for V-polarization at 12 GHz, although measured gain is 1.2 dB lower than the simulated value obtained when using the nominal values of ε_r and tanδ at 10 GHz provided by the manufacturer. Similar results are obtained for the other polarization and the other frequencies of Ku-band, although they are not shown here. However, the comparison between simulated and measured radiation patterns in Ka-band showed stronger disagreements than in Ku-band. It was checked that the tolerance errors in the lengths and widths of the dipoles (an average increment of 50 μm) were not large enough to justify the differences. The bonding film (CuClad 6250 with $\varepsilon_r = 2.32$ and tan$\delta = 0.0013$), which had been originally neglected in the design of the antenna because of its small thickness (38 μm), was also considered in the simulations by the inclusion of a new dielectric layer between layers A and B. As a result, slight differences were detected in the radiation patterns, but they were not sufficient to justify the difference between measured and simulated gain in Ka-band. In order to find the explanation for this disagreement, the dielectric constant and loss tangent of

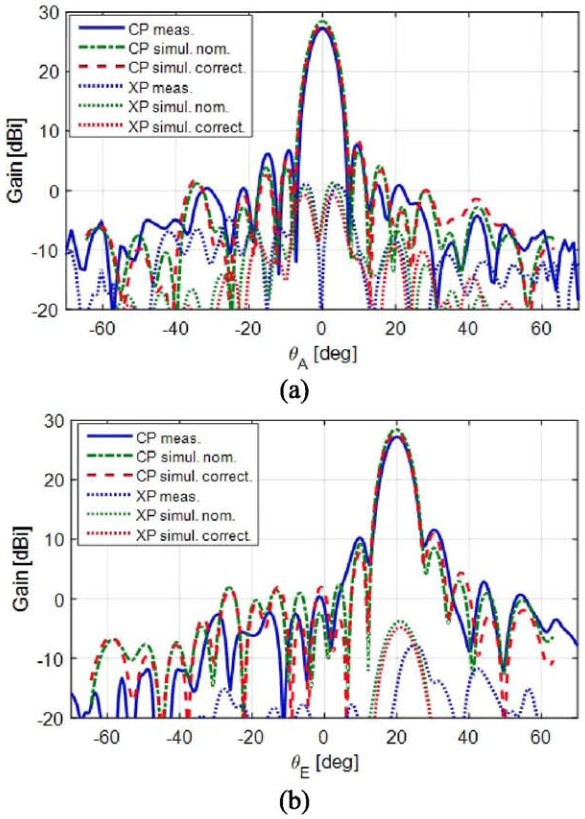

Fig. 7. Measured and simulated radiation patterns at 12 GHz for V-polarization in (a) azimuth and (b) elevation planes.

both substrates were measured by means of the technique described in [16]. The results showed that the dielectric constant in Ka-band is always larger than the nominal values provided by the manufacturer. For AD255C, $\varepsilon_{rA} = 2.70$ was measured, instead of $\varepsilon_{rA} = 2.55$, and for Diclad 880, $\varepsilon_{rB} = 2.30$ was measured, instead of $\varepsilon_{rB} = 2.17$. The measured loss tangent is also larger than the nominal values: tanδ close to 0.005 was measured for both substrates, instead of 0.0009. Therefore, additional simulations were carried out by taking into account the measured values of permittivity and loss tangent of layers A and B. As a consequence, the corrected radiation patterns in Ka-band showed a better correspondence with experimental results, while the patterns in Ku-band presented a slight reduction in gain. The amplitude and phase response of the cell was also analyzed considering the corrected values of ε_r and tanδ, and the results are included in Fig. 2, superimposed to the curves obtained with nominal values of ε_r and tanδ. As can be seen, the worst effects occur in Ka-band, where the losses can be several times larger than originally expected. Moreover, significant phase errors appear in those elements with upper central dipoles larger than 5.5 mm, these errors being responsible for the deterioration of the radiation patterns.

Finally, it has been found that there are a few cells near the edge of the reflectarray, for which the first higher order Floquet mode starts propagating at higher frequencies, which is the condition for grating lobe appearance. We have modified our software tool to take into account the contribution of higher order Floquet harmonics in the radiated field and we have analyzed again the antenna. The simulated corrected patterns considering the measured values of ε_r and tanδ and the effect of higher order Floquet modes are shown in Figs. 7 and 8. A slightly better agreement between simulations and measurements (not included in the figures) was found after

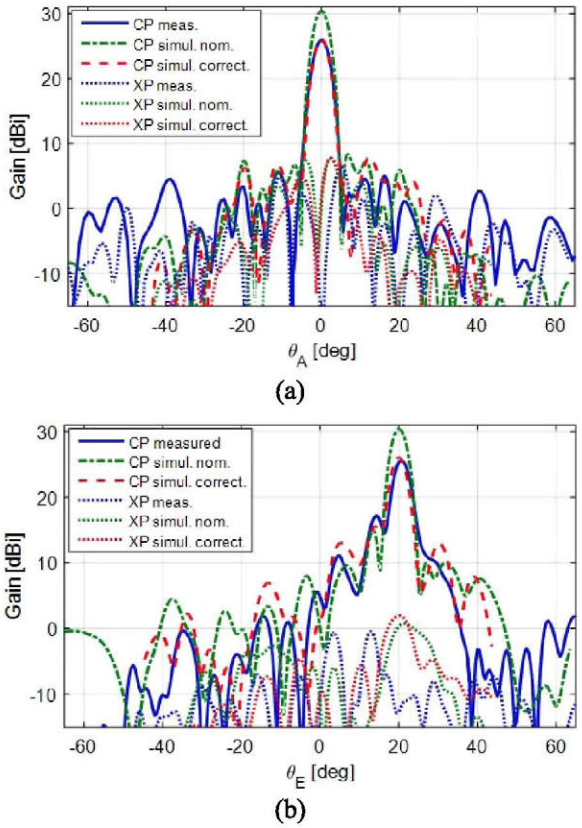

Fig. 8. Measured and simulated radiation patterns at 19.5 GHz for H-polarization in (a) azimuth and (b) elevation planes.

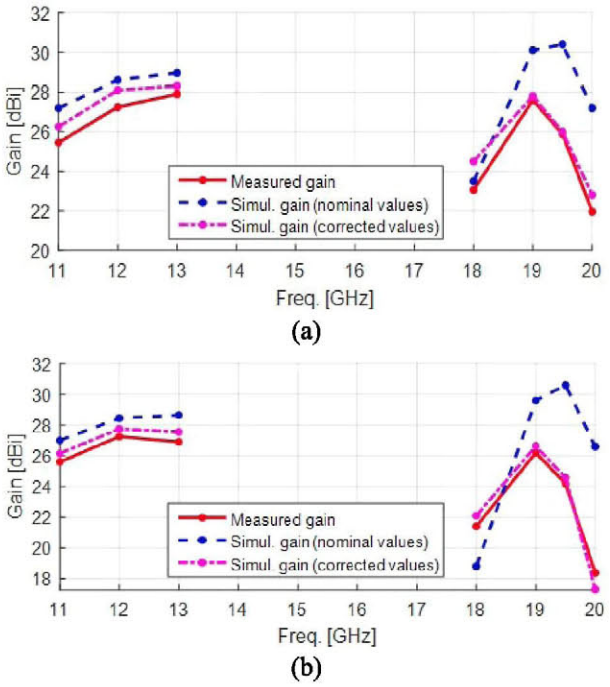

Fig. 9. Measured versus simulated gain graphs in Ku- and Ka-bands for (a) H-polarization and (b) V-polarization.

inclusion of higher order Floquet modes. However, the main source of discrepancies between original simulations and measurements is not the excitation of grating lobes, but the difference between nominal and measured values of ε_r and tanδ in the materials. The bad initial estimation of the dielectric constant of the substrate layers shifted the antenna operation in the upper band to lower frequencies (from 19–20 GHz to around 18.5–19.5), while the higher measured loss tangent also had an effect on reducing the antenna gain, especially in Ka-band. The inclusion of the aforementioned correction factors in the simulations contributes to obtain a better agreement with the measurements, causing a reduction in gain and an increase of sidelobes, as can be seen in the patterns.

TABLE I
COMPARISON OF MAIN ANTENNA PARAMETERS

Freq. (GHz)	SLL meas. (dB)	SLL corrected (dB)	SLL nominal (dB)	XPD meas. (dB)	XPD corrected (dB)	XPD nominal (dB)
			Pol. H			
11	13.40	13.71	13.60	21.48	22.31	24.62
12	13.65	17.75	16.51	23.82	22.07	24.79
13	14.15	17.18	18.12	24.03	22.19	26.73
19	16.50	16.34	17.58	21.66	21.36	24.51
19.5	8.47	10.47	15.40	26.18	14.92	19.54
20	2.41	5.34	10.63	18.78	14.43	15.53
			Pol. V			
11	16.02	14.53	13.92	28.85	27.87	27.45
12	15.59	16.84	19.23	24.25	25.52	24.31
13	12.90	17.42	18.59	23.47	25.82	25.58
19	12.03	17.76	14.55	18.67	21.12	22.40
19.5	7.48	7.71	20.25	18.98	16.54	19.49
20	0.12	0.39	10.55	14.02	11.24	18.59

Fig. 9 shows the evolution of gain with frequency in each polarization for both measurements and simulations, while considering the nominal values of ε_r and tanδ of the two dielectric materials, as well as the corrected values. As can be seen, there is a shift in the frequency response in Ka-band (the maximum gain is measured at 19 GHz, instead of at 19.5 GHz). It can be also observed that the manufactured demonstrator is wideband in the lower band (roughly 20% bandwidth for a gain variation smaller than 2 dB) and narrow band in the upper band (around 5% bandwidth for a gain variation smaller than 2 dB). Moreover, the values of sidelobe level (SLL) and cross-polar discrimination (XPD) of the antenna radiation patterns are summarized in Table I for simulations and measurements. The radiation patterns and antenna gain should be improved by using the real properties (extracted from measurements) of the materials at the operation frequencies in the design process.

V. CONCLUSION

A 25-cm reflectarray prototype, capable of operating in the transmit frequencies (from a satellite) in Ku-band (11–13 GHz) and Ka-band (19–20 GHz), has been designed, manufactured, and measured as a proof-of-concept to demonstrate the independent operation in two frequencies and two polarizations with separate feeds. The reflectarray cell is composed of two orthogonally arranged sets of coupled parallel dipoles, which are distributed in a two-level configuration. The results show a quite good agreement with the simulations in Ku-band, and some discrepancies at Ka-band due to a variation in the electrical properties of the materials (dielectric constant and loss tangent). To avoid this problem, the materials should be accurately characterized before carrying out the design of the antenna. This concept can be applied to transmit satellite antennas to reuse the same aperture for the generation of a prescribed contoured beam in Ku-band and multiple spots in Ka-band with different feed chains for each mission, leading to significant savings in the cost, volume, and weight of the antenna farm in communications satellite systems.

REFERENCES

[1] J. Huang and J. A. Encinar, *Reflectarray Antennas*. Piscataway, NJ, USA: IEEE Press, 2008.

[2] W. A. Imbriale, S. Gao, and L. Boccia, *Space Antenna Handbook*. Hoboken, NJ, USA: Wiley, 2012.

[3] H. Fenech, A. Tomatis, D. Serrano, E. Lance, and M. Kalama, "Spacecraft antenna requirements as perceived by an operator," *IEEE Antennas Propag. Mag.*, vol. 53, no. 5, pp. 256–266, Oct. 2011.

[4] R. Orr *et al.*, "Circular polarization frequency selective surface operating in ku and Ka band," *IEEE Trans. Antennas Propag.*, vol. 63, no. 11, pp. 5194–5197, Nov. 2015.

[5] J. A. Encinar *et al.*, "Dual-polarization dual-coverage reflectarray for space applications," *IEEE Trans. Antennas Propag.*, vol. 54, no. 10, pp. 2827–2837, Oct. 2006.

[6] T. Smith, U. V. Gothelf, O. S. Kim, and O. Breinbjerg, "Design, manufacturing, and testing of a 20/30-GHz dual-band circularly polarized reflectarray antenna," *IEEE Antennas Wireless Propag. Lett.*, vol. 12, pp. 1480–1483, 2013.

[7] R. Deng, Y. Mao, S. Xu, and F. Yang, "A single-layer dual-band circularly polarized reflectarray with high aperture efficiency," *IEEE Trans. Antennas Propag.*, vol. 63, no. 7, pp. 3317–3320, Jul. 2015.

[8] J. A. Encinar, "Design of a dual frequency reflectarray using stacked patches of variable size," *Electron. Lett.*, vol. 32, no. 12, pp. 1049–1050, Jun. 1996.

[9] M. R. Chaharmir, J. Shaker, and H. Legay, "Dual-band Ka/X reflectarray with broadband loop elements," *IET Microw. Antennas Propag.*, vol. 4, no. 2, pp. 225–231, Feb. 2010.

[10] M. R. Chaharmir and J. Shaker, "Design of a multilayer X-/Ka-band frequency-selective surface-backed reflectarray for Satellite applications," *IEEE Trans. Antennas Propag.*, vol. 63, no. 4, pp. 1255–1262, Apr. 2015.

[11] R. Florencio, J. A. Encinar, R. R. Boix, V. Losada, and G. Toso, "Reflectarray antennas for dual polarization and broadband telecom Satellite applications," *IEEE Trans. Antennas Propag.*, vol. 63, no. 4, pp. 1234–1246, Apr. 2015.

[12] E. Martinez-de-Rioja, J. A. Encinar, R. Florencio, and R. R. Boix, "Dual polarized reflectarray antenna to generate independent beams in Ku and Ka bands," in *Proc. 10h Eur. Conf. Antennas Propag.*, Davos, Switzerland, Apr. 2016, pp. 1–5.

[13] E. Martinez-de-Rioja, J. A. Encinar, R. Florencio, and R. R. Boix, "Reflectarray in K and Ka bands with independent beams in each polarization," in *Proc. IEEE Int. Symp. Antennas Propag.*, Fajardo, PR, USA, Jul. 2016, pp. 1199–1200.

[14] D. Martinez-de-Rioja, E. Martinez-de-Rioja, and J. A. Encinar, " Multibeam reflectarray for transmit Satellite antennas in Ka band using beam-squint," in *Proc. IEEE Int. Symp. Antennas Propag.*, Fajardo, PR, USA, Jul. 2016, pp. 1421–1422.

[15] R. Florencio, R. R. Boix, E. Carrasco, J. A. Encinar, and V. Losada, "Efficient numerical tool for the analysis and design of reflectarrays based on cells with three parallel dipoles," *Microw. Opt. Technol. Lett.*, vol. 55, no. 6, pp. 1212–1216, Jun. 2013.

[16] B. Bianco and M. Parodi, "Measurement of effective relative permittivities of microstrip," *Electron. Lett.*, vol. 11, no. 3, pp. 71–72, 1975.